IV Journeys in Multiphase Flows (JEM 2015)
March 23-27, 2015, Campinas, SP, Brazil

Paper ID: JEM-2015-XXXX

IMPROVEMENT OF DISPERSED OIL-WATER PIPE FLOW IMAGES

Adriana Bonilla Riaño
University of Campinas and Cidade Universitaria-B. Geraldo, Cx.P. 6122, 13083-970, Campinas, SP, Brazil
adriana@dep.fem.unicamp.br

Oscar M.H. Rodriguez
University of Sao Paulo and Av. Trabalhador São Carlense, 400, 13566-970 São Carlos, SP, Brazil
oscarmhr@sc.usp.br

Abstract. *In this paper dispersed oil-in-water flow images were improvement, as a pre-processing step for the water film thickness estimation. The images have noise and low contrast, which makes any image processing difficult. So different methods for image enhancement were reviewed, implemented and compared using some image quality metrics. Based on the studied methods a new methodology was proposed. The new methodology has three steps, in the following sequence: noise reduction using Wavelet denoising, deblurring using an unsharp filtering and contrast enhancement with contrast limited adaptive histogram equalization. The proposed method produces better results than the individual methods in terms of the metric and the visual result.*

Keywords: *Dispersed oil-water pipe flow, image processing, denoising, spatial filtering, frequency filtering, contrast improvement.*

1. INTRODUCTION

Liquid-liquid flow is commonly encountered in the petroleum industry, where a number of applications involve oil-water flow such as crude oil production and transportation. The water proportion in crude oil production is increasing day by day and then the flow of oil-water mixtures is receiving more attention from the researchers. In oil transportation process the flow of a mixture of oil and water through pipelines over long distances causes significant pressure losses. The co-current pipe flow of two liquids is more complex as compared to single-phase flow of either of the fluids and the prediction of the frictional pressure gradient usually cannot be made by extrapolation of single-phase codes. The proper design of a two-phase production well or pipeline depends on the accurate prediction of this frictional pressure gradient.

The oil-water dispersed flow pattern, where the oil is dispersed as droplets into the water, is common in crude oil transmission and offshore pipelines. However it has not been studied as intensively as separated or intermittent flows. An interesting feature of this kind of pattern flow is the drag reduction phenomenon, yet not well understood. The drag reduction phenomenon can be defined as a reduction in two-phase pressure gradient when compared to single-phase equivalent values. The occurrence of drag reduction phenomenon without the addition of drag reduction agents in dispersed flow has been reported in some works (Angeli and Hewitt, 1998; Ioannou et al., 2005; Lovick and Angeli, 2004; Omer and Pal, 2010; Pal, 2007). For instance, I. H. Rodriguez (Rodriguez et al., 2011) observed a reduction of up to 25% of two-phase pressure gradient with respect to the corresponding single-phase water pressure gradient at the same mixture velocity in a viscous oil-water dispersed flow. A phenomenological model that assumes the existence of a thin water film adjacent to the pipe wall was proposed to explain the drag-reduction mechanism, but it lacks experimental confirmation. In this context, one may notice that the experimental investigation of liquid-liquid flows, especially oil-water flow, is growing because of the industrial relevance. However, more research into the physics of liquid-liquid flow is necessary.

In this paper dispersed oil-in-water flow images were processed, the aim of the experimental work was to confirm the existence of a water film and measure the water film thickness using a high speed camera. The first stage of that task was to improve images, because the dispersed oil-in-water flow images have noise and low contrast, which makes the processing image difficult. The purpose of image enhancement is to improve the interpretability of information contained in the image for providing a "better" input for other automated image processing systems (Kaur et al., 2011). It is important to remark that many image enhancement methods have been proposed nevertheless they are not suitable for all the cases. It is necessary to make a particular study for each case, having into account its characteristics and purpose, regularly a certain amount of trial and error is required before a particular image enhancement approach is selected (Gonzales and Woods, 2002).

2. METODOLOGY

2.1 Experimental setup

The images were recorded with a high-speed video camera (Olympus ispeed3, at 5000 fps) in the Multiphase-Flow-Loop Test Facility of LETeF (Thermal-Fluids Engineering Laboratory), Engineering School of São Carlos of the University of São Paulo. The camera was installed at 10.3m from the tube entrance of a horizontal transparent acrylic pipeline of 26 mm-i.d. and 12 m length, **Erro! Fonte de referência não encontrada.**. Tap water and oil ($828\ \mathrm{kg/m^3}$ of density and 220 mPa s) were used as test fluids.

The experimental procedure started with single-phase water flow. After some time, oil was gradually added. After reaching steady state, the high-speed camera was activated. **Erro! Fonte de referência não encontrada.** (b and c) shows frames for two experiments with different oil and water superficial velocities (Uos, Uws). It is possible to observe a small region at the top of the pipe, near to the wall, free of the oil droplets; it is the studied water film.

A total of 14 experiments on dispersed flow were recorded for water superficial velocities varying from 1.2 to 3.0 m/s and input oil fractions from 0.14 to 0.48.

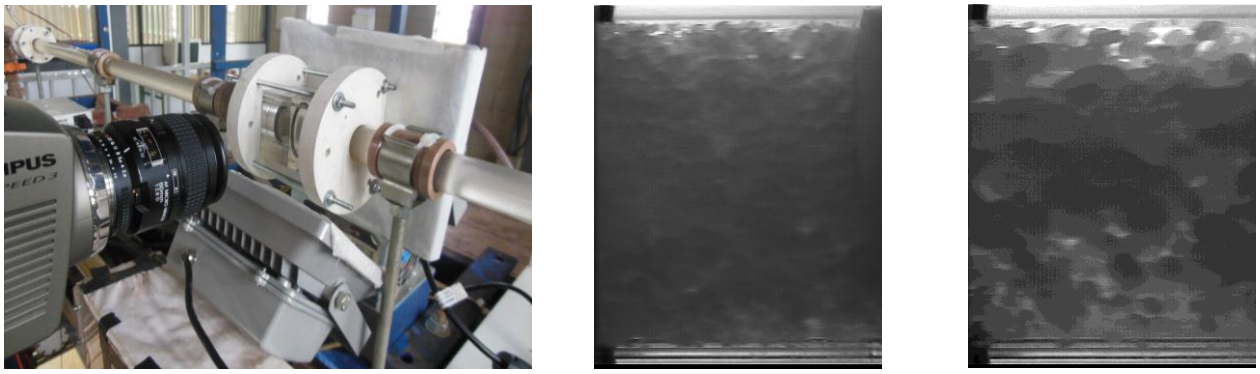

a) b) c)

Figure 1. a) Camera experiments setup. Images dispersed oil in water flow pattern; (b) Uws=3.0 m/s, Uos=1.2 m/s; c) Uws=250 m/s, Uos=0.8 m/s

2.2 Image enhancement

The image enhancement algorithm receives an original image, applies a set of intermediate steps on that image, and finally outputs the enhanced image. There are many techniques for improving image quality. Some popular techniques are contrast improvement, edge enhancement (e.g. deblurring), spatial (e.g. averaging, median, Wiener, frost filters) and frequency filtering (Fourier and Wavelet domain).

2.2.1 Contrast improvement

Dispersed oil-in-water flow images have non-uniform illumination and low contrast, having necessary to improve those before any processing. Contrast enhancement techniques expand the range of brightness values in an image thus the effect is to increase the visual contrast between two areas of different uniform densities. For this objective was selected a histogram based contrast improvement.

Given a gray scale image with L levels of intensity the intensity gray histogram is defined as a function $h(g)$ which value for each intensity level $g \in [0 \ldots . L]$, is the number of pixels in the image N_g that have intensity equal to g.

$$h(g) = N_g \tag{1}$$

Histograms are frequently normalized by the total number of pixels in the image. Assuming an M × N image, a normalized histogram is:

$$p(g) = \frac{N_g}{MN} \tag{2}$$

where $p(g)$ is the probability of occurrence of g in the image. The sum of all components of a normalized histogram is equal to 1.

The histogram of a low contrast image is usually skewed either to the left (mostly light), to the right (mostly dark), or located around the right (mostly gray). In our case, Figure 3, the values are around the right side.

Contrast stretching is a point image enhancement method that attempts to improve an image by stretching the range of intensity values it contains to make full use of possible values. Contrast stretching is restricted to a linear mapping of input to output values. A disadvantage of the method of histogram stretching is that they require user input. This method was not used in this case because it is non-practical to study each histogram to estimate the lower and upper gray levels (we have 70000 images).

On Histogram Equalization (HE) the pixel value of enhanced image depends on global pixel value of the origin image. Actually, it is the probability density function (pdf) that will be transformed, i.e. it changes the pdf of a given image into one of a uniform pdf that spreads out from the lowest pixel value to the highest pixel value (L– 1). In a digital image, the pdf is a discrete function and can be approximated using the probability based on the histogram p(g) as follows:

$$pdf(x) = p(g) = \frac{N_g}{MN} \tag{3}$$

From this pdf, we can then obtain the cumulative density function (cdf) as follows:

$$\text{cdf(x)} = \sum_{g=0}^{L-1} p(g) \tag{4}$$

The transformed pixel can be obtained by:

$$t = \text{floor}(cfd(x)\ (L-1)) \tag{5}$$

where Floor rounds to the nearest integer (Bagade and Shandilya, 2011).

HE can be a good approach when automatic enhancement is required, even though there are cases where basing image enhancement on a uniform histogram may not be the best approach, causing results excessively strong (Singh et al., 2011).

Contrast Limited Adaptive Histogram Equalization (CLAHE) is different to the previous histogram equalization because the method computes several histograms, each corresponding to a distinct region of the image, and applies the histogram equalization to each one, with a defined distribution. The objective of process is to improve the local contrast of an image.

The method utilizes a parameter limit value of histogram in order to obtain adequate brightness and contrast on the enhanced image. The contras limit is controlled on the histogram equalization process. Criterion of desired histogram distribution is defined based on contrast range of original image. Some criterion of form of histogram distribution is uniform, exponential, or Rayleigh. Therefore, the natural property of original image can be maintained since the distribution form is not significant change after enhancement process (Juliastuti and Epsilawati, 2012).

2.2.2 Denoising

Noise is any degradation in the image signal, caused by external disturbance. Digital images may be contaminated by a variety of types of noise. Noise is the result of errors in the image acquisition process that result in pixel values that do not reflect the true intensities of the real scene. Generally, noisy pixels appear as dots with different gray levels to its neighborhood. These points appear random or distributed systematically. Image noise can be classified as impulse noise, Gaussian noise, Poisson noise, quantization noise, film grain, on-isotropic noise, multiplicative noise and periodic noise (Verma and Ali, 2013). Following are described some noises that can contaminate dispersed oil-in-water flow images.

In impulse noise or salt and pepper noise, the noise arises in the image because of sharp and sudden changes of image signal. In this type of noise only two values are possible, a and b, and the probability of obtaining each of them is less than 0.1. For instance in an 8 bits image, the typical value for pepper noise is close to 0 and for salt is close to 255.

Gaussian or amplifier noise is caused by random fluctuations in the signal. Some sources of Gaussian noise are: different gains in the sensor, electrical noise in the digitizers, poor illumination and high temperature, between others. The Gaussian noise has a normal probability distribution function, i.e., the values that the noise can take on are Gaussian-distributed.

Poisson or shot photon noise arises when the number of photons sensed by the sensor is not sufficient to provide detectable statistical information. This noise has root mean square value proportional to square root intensity of the image.

Noise reduction (denoising) in digital images has been studied for many years. Image denoising methods can be categorized as either spatial domain methods or transform domain methods. Spatial domain methods suppress noise directly in the spatial domain (e.g., spatial filtering). Transform domain methods first transform an image from the spatial domain into a different domain (e.g., frequency domain, wavelet domain) and suppress noise in the transform domain (Gonzales and Woods, 2002). According to noise nature and its characteristics, a given denoising method can be more effective than another. Some of these methods are presented below.

Spatial filtering techniques are transformations pixel by pixel, depending not only on the gray level of the pixel, but also on the value of the gray levels of neighboring pixels. The filtering process is performed using masks, which are applied on the image. Applying the mask centered at the pixel $P(i,j)$, where i is the row number and j the column number in the image, means to replace the pixel value at position (i,j) for a new value, where the value depends on the values of neighboring pixels and weights on the mask. Examples of such filters are averaging filters, median filters and adaptive filters.

Averaging filters replace each pixel value in an image with the average value of its neighbors, including itself. This has the effect of eliminating pixel values which are unrepresentative of their surroundings. The result will depend on the window size, i.e., the number of pixels averaged. Its implementation can be generalized as the sum of the pixel values in the region multiplied by a set of mask weights ($W_{x,y}$), Eq. (6). This process results in an image with reduced "sharp" transitions in gray levels and less noise because random noise typically consists of sharp transitions in gray levels. Nevertheless, edges (which almost always are desirable features of an image) also are characterized by sharp transitions in gray levels, so averaging filters have the undesirable side effect that they blur edges.

$$P(i,j) = \sum_{x,y=-m}^{m} W_{x,y} P_{x+i,y+j} \tag{6}$$

where m represents the size of the mask, P is the pixel value.

In median filters, the gray level of each pixel is replaced by the median of the gray levels in the neighborhood. For example, in a neighborhood of 3×3 pixels, the median is the fifth largest value; in a neighborhood of 5×5 pixels is the thirteenth largest value, and so on. Median filter is good for salt and pepper noise. The median filter can eliminate the effect of input noise values with extremely large magnitudes. These filters are widely used as smoothers in image processing (Gonzales and Woods, 2002).

An adaptive filter changes its behavior on the basis of statistical characteristics of the image region, encompassed by the filter region. This approach produces good results preserving edges and other high frequency parts of an image. In this work a Wiener filter (Jin et al., 2003) and a frost filter (Yu and Acton, 2002) were used.

Another important method of noise reduction is the technique known as "wavelet shrinkage". This method was originally proposed by Donoho and Johnstone (Donoho and Johnstone, 1994) and applied by many authors to reduce noise in signals and images (Ergen, 2012; Luisier et al., 2007).

The wavelet transform is basically a convolution operation, which is equivalent to passing an image through low-pass and high-pass filters. The low frequency image or low frequency sub-band (SLL) still contains spatial correlation and by filtering recursively the SLL a multi-resolution image representation can be obtained. Thus, the image is decomposed into a set of sub-images with different resolutions for different frequency bands. Most of the wavelet detail coefficients are equal or close to zero in the regions of smooth image intensity variation.

Wavelet denoising consists of three main stages:

1. Perform a discrete wavelet transform (DWT) to the noisy image.
2. Application of threshold, in order to suppress coefficients due to noise.
3. Reconstruct the denoised image by applying the inverse discrete wavelet transform (IDWT) on the processed highpass wavelet subimages to obtain an estimate of the noise-free image.

Wavelet denoising method relies on the fact that noise commonly manifests itself as fine-grained structure in the image and DWT provides a scale based decomposition. Consequently, most of the noise tends to be represented by wavelet coefficients at the finer scales. Eliminating these coefficients would result in a natural filtering of the noise on the basis of scale. Because the coefficients at such scales also tend to be the primary carriers of edge information, this method threshold the DWT coefficients to zero if their values are below a threshold. These coefficients are mostly those corresponding to noise. The edge relating coefficients on the other hand, are usually above the threshold (Arivazhagan et al., 2007). There are some variables in the research of the wavelet denoising on images to be studied; the wavelet function and the level N of wavelet decomposition, the wavelet thresholding function and the threshold.

2.2.3 Deblurring

Denoising reduces the noise level but the resultant image could be blurred or over smoothed due to losses like edges or lines. Unsharp filter was selected to deblurring the images after denoising step. The unsharp filter enhances edges (and other high frequency components in an image) via a procedure which subtracts an unsharp, or smoothed, version of an image from the original image (Gonzales and Woods, 2002).

3. RESULTS

In total, 70000 images were improved. First, each method presented in the Image enhancement section was applied to the images to compare their results and select the best technique.

The performance of image enhancement methods can be evaluated using quality metrics. Given an original image x_o with N columns and M rows, after an enhancement process is obtained an improved image x_e with the same size. The quality parameters used in this paper are in Table 1 (Pavithra et al., 2010).

Table 1. Quality metrics used to compare the enhancement methods.

Metric	Definition	Equation	Better quality if
Mean Squared Error (MSE)	Global difference between an enhanced image and an original image.	$MSE = \frac{1}{NM}\sum_{0}^{N-1}\sum_{0}^{M-1}(x_o(n,m) - x_e(n,m))^2$	Low value
Mean Average Error (MAE)	Average magnitude of the errors.	$MAE = \frac{1}{NM}\sum_{0}^{N-1}\sum_{0}^{M-1}\lvert x_o(n,m) - x_e(n,m)\rvert$	Low value
Peak Signal to Noise Ratio (PSNR)	Comparison between noise and signal peak. The unit of PSNR is dB (decibel).	$PSNR = 20\log_{10}\left(\frac{255}{MSE}\right)$	High value
Structural Correlation (SC)	Similarity of the structure of two images.	$SC = \frac{\sum_{0}^{N-1}\sum_{0}^{M-1}(x_o(n,m))^2}{\sum_{0}^{N-1}\sum_{0}^{M-1}(x_e(n,m))^2}$	Low value
Maximum Difference (MD)	Maximum of the difference between original and enhanced image.	$MD = \max(\lvert x_o(n,m) - x_e(n,m)\rvert)$	Low value
Contrast	Comparison between original and enhanced image contrast.	$Contrast = \frac{\frac{1}{NM}\sqrt{\sum_{0}^{N-1}\sum_{0}^{M-1}\lvert x_e(n,m) - Mean_e\rvert}}{\frac{1}{NM}\sqrt{\sum_{0}^{N-1}\sum_{0}^{M-1}\lvert x_o(n,m) - Mean_o\rvert}}$ where Mean is the global mean.	High value

3.1 Contrast enhancement results

Histogram equalization and contrast limited adaptive histogram equalization were tested. The results of image enhancement of the same image with several methods and also plot of histogram distribution are showed on Figure 2 and Figure 3.

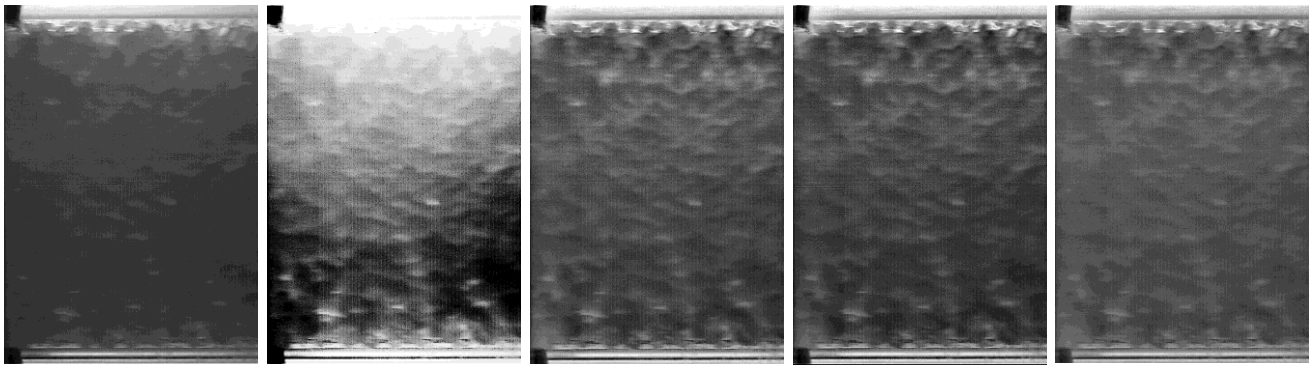

a) b) c) d) e)

Figure 2. Original image Uws=2.5 m/s, Uos=1.2 m/s; b) Image after HE; Image after CLAHE with: c) Uniform distribution; d) Exponential distribution; e) Rayleigh distribution

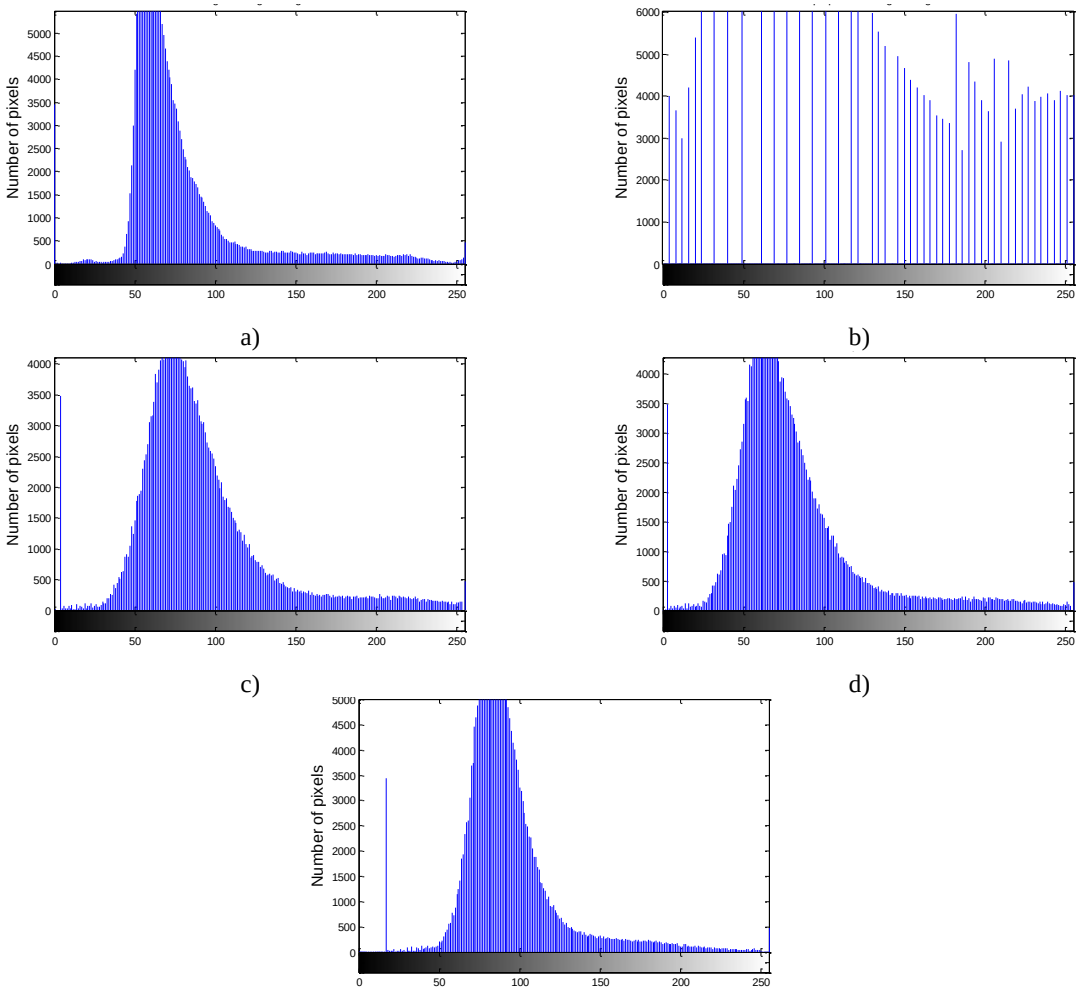

Figure 3. Histogram of original image Uws=2.5 m/s, Uos=1.2 m/s; b) Histogram after HE; Histogram after CLAHE with: c) Uniform distribution; d) Exponential distribution; e) Rayleigh distribution

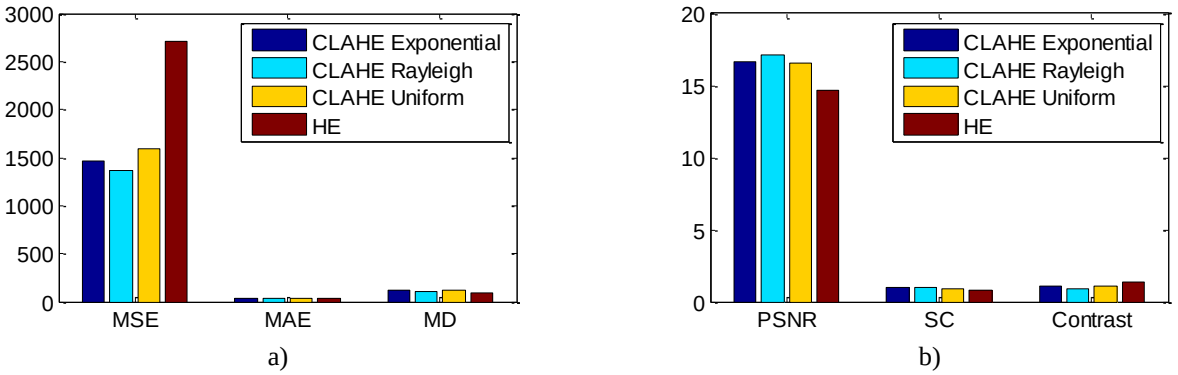

Figure 4. Mean of image quality metrics for different methods of contrast improvement; a) MSE, MAE and MD; b) PSNR, SC and Contrast

According to the quality metrics the best method for contrast improvement for the tested images was CLAHE with Rayleigh distribution. CLAHE with Rayleigh have better values in MSE, MAE, MD and PSNR, following by CLAHE with exponential distribution, Figure 4.

3.2 Noise reduction results

The results of applying filters to one image are shown in Figure 5. It was focused on the top of the image, because our interest is to measure the water film thickness. The filters were implemented with masks of $3x3$ and $5x5$ pixels.

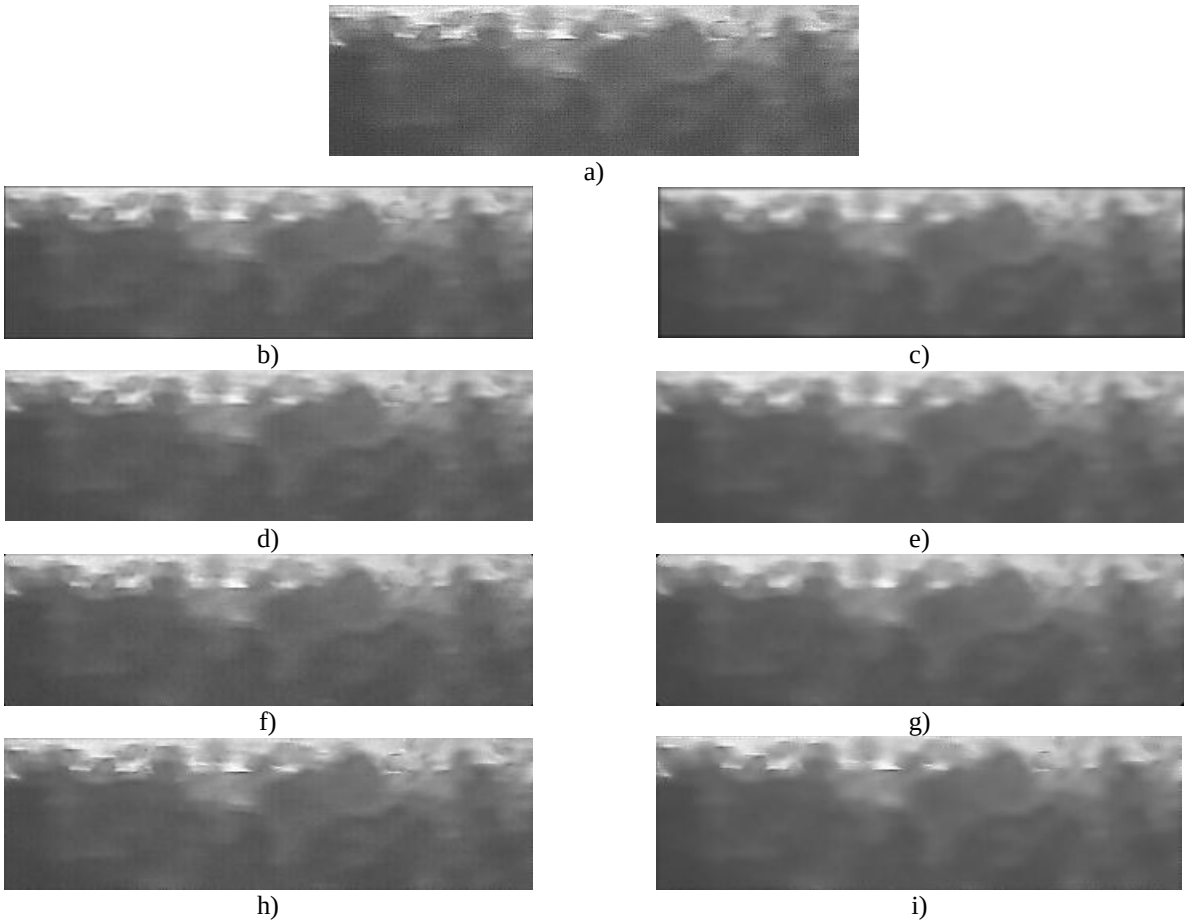

Figure 5. Visual enhancement results of different algorithms for one image Uws=2.5 m/s, Uos=1.2 m/s; a) Original image; b) Averaging filter 3x3; c) Averaging filter 5x5; d) Frost filter 3x3; e) Frost filter 5x5; f) Median filter 3x3; g) Median filter 5x5; h) Wiener filter 3x3; i) Wiener filter 5x5

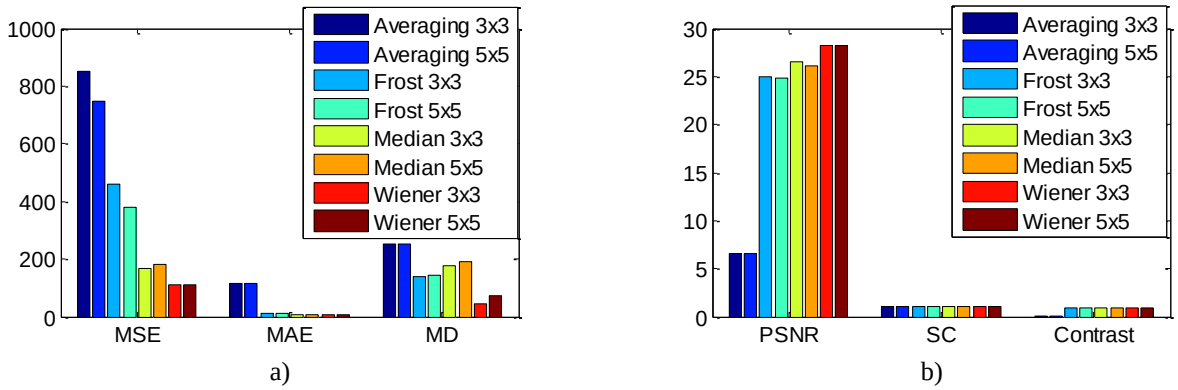

Figure 6. Mean of image quality metrics for different filters; a) MSE, MAE and MD; b) PSNR, SC and Contrast

Due to spatial filters employ a low pass filtering on groups of pixels, with the assumption that the noise occupies the higher region of frequency spectrum, not only smooth away noise but also blur edges in the images (Figure 5). This blur increases with the mask size. It can be seen that correlation between image characteristic related with performance of image enhancement method is close (Figure 5 and Figure 6). In this case, the best tested filtering method was Wiener filter with mask of 3x3.

A series of steps were made to find the best combination of parameters for Wavelet noise reduction. First, different Wavelets functions were compared. Those Wavelet functions were: Haar, Daubechies (db) from 2 to 40, Symlets (sym) from 1 to 8, Coiflets (coif) from 1 to 5, biorthogonal (bior) from 1.1 to 6.8 and reverse biorthogonal (rbio) from 1.1 to 6.8. Noise reduction was performed with WDT with two-level decomposition and the soft Rigrsure threshold. In the second step were tested different levels of decomposition (1 to 40), using the best Wavelet function found in the previous step and at last were compared two classical thresholds (soft threshold and hard threshold). The main image quality metric was PSNR. Figure 7 shows Wavelet denoising results with different Wavelet functions, on the top are presented the best cases and immediately after the worst cases, chosen by their PSNR.

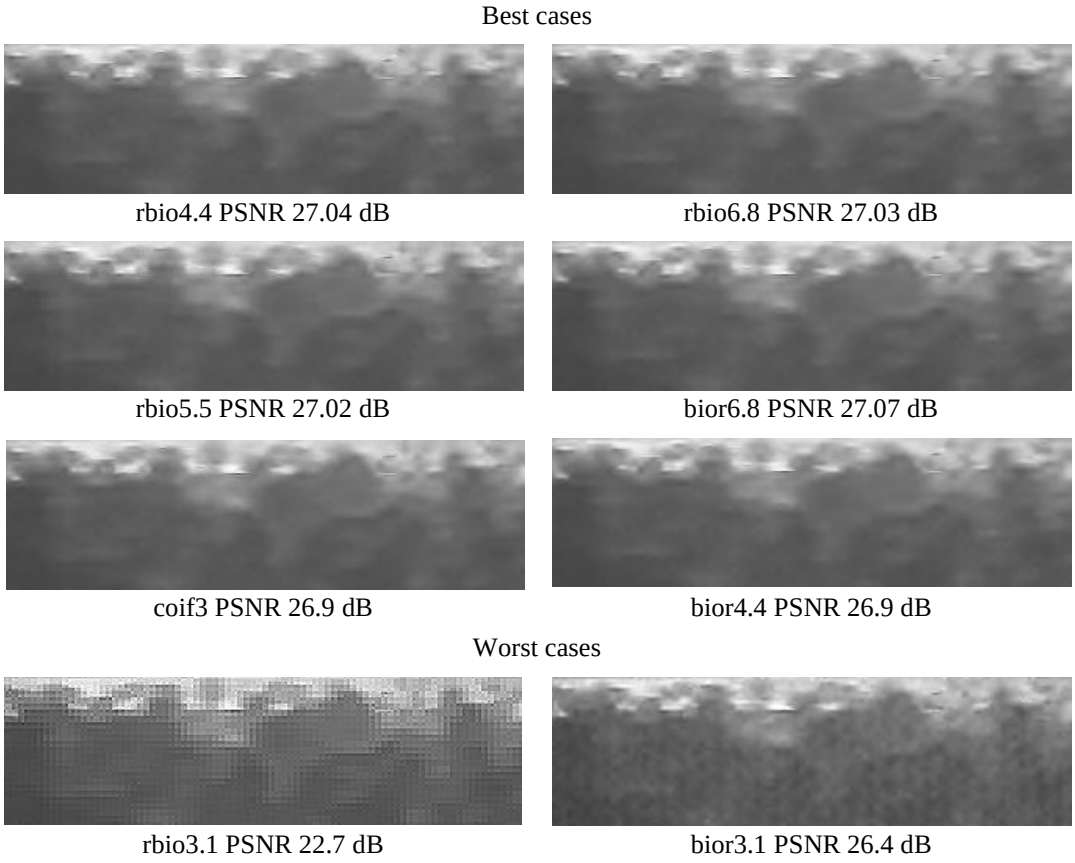

Figure 7. Visual enhancement results of wavelet denoising using different Wavelet functions for one image Uws=2.5 m/s, Uos=1.2 m/s

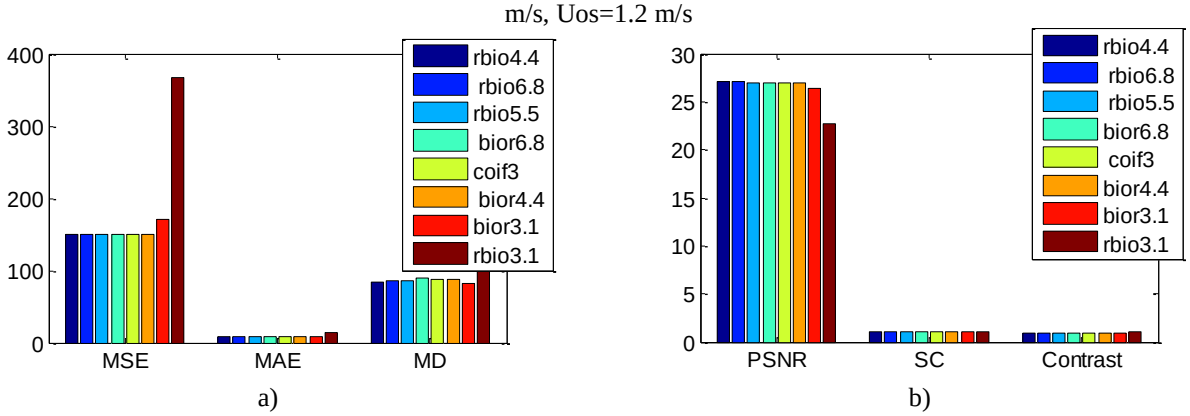

Figure 8. Mean of image quality metrics for different Wavelet; a) MSE, MAE and MD; b) PSNR, SC and Contrast

Table 2. Mean of image quality metrics for different levels and thresholds.

Levels	MSE	MAE	PSNR	SC	MD	Contrast
1	121.72	7.68	27.98	1.015	73.07	0.984
2	149.13	8.32	27.03	1.019	83.55	0.981
3	162.36	8.68	26.60	1.022	86.65	0.979
4	170.99	8.98	26.35	1.026	88.02	0.976
5	175.18	9.14	26.24	1.028	87.62	0.973
Threshold						
Hard	111.72	7.42	28.40	1.013	55.75	0.985
Soft	121.72	7.68	27.98	1.015	73.07	0.984

In accordance to the results of the image quality metrics MSE, MAE, PSNR, SC and MD (Figure 8 and Table 2), the best parameters for Wavelet denoising are: Wavelet function reverse biorthogonal 4.4 (rbio4.4), one decomposition level and threshold hard. In Figure 9 is presented a Wavelet denoising result to an image. It has been found that wavelet based denoising is effective in noise reduction with edge features without much damage.

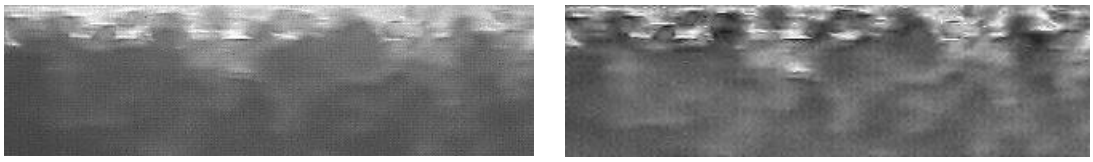

a) b)

Figure 9. Visual enhancement results of Wavelet denoising for one image Uws=2.5 m/s, Uos=1.2 m/s; a) original image; b) Denoised image

3.3 Deblurring

An example of application of unsharp filtering is presented in Figure 10. Visual enhancement results of unsharp filtering for one image Uws=2.5 m/s, Uos=1.2 m/s; a) original image; b) enhancement imageFigure 10.

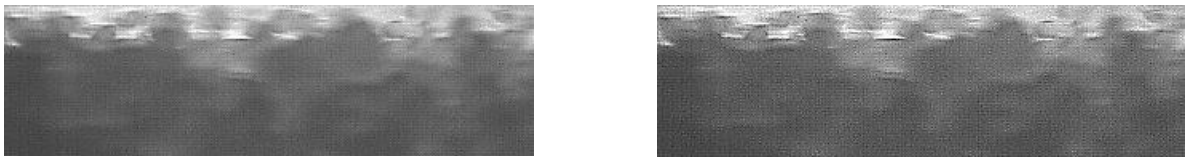

a) b)

Figure 10. Visual enhancement results of unsharp filtering for one image Uws=2.5 m/s, Uos=1.2 m/s; a) original image; b) enhancement image

3.4 Proposed algorithm

Subsequent to have the outcome of every technique is necessary to determine how will be the sequence of the algorithm for improving dispersed oil-in-water flow images. The proposal is to use the best proven techniques combined. The possible combination were implemented and compared. The techniques combined were CLAHE with Rayleigh distribution (Contrast in Figure 11), Wavelet denoising with rbio4.4 Wavelet, one decomposition level and hard thresholding (Denoising in Figure 11) and unsharp filter (Unsharp in Figure 11). The most favorable option is appliying the techniques in the sequence Wavelet denoising, unsharp filtering and CLAHE with Rayleigh distribution (orange in Figure 11). The proposed combination has the lowest values of MSE, MAE, MD; the highest PSNR and the visual result is better than using an single method, Figure 12. Finally, the flowchart of the proposed enhancement algorithm is shown in Figure 13.

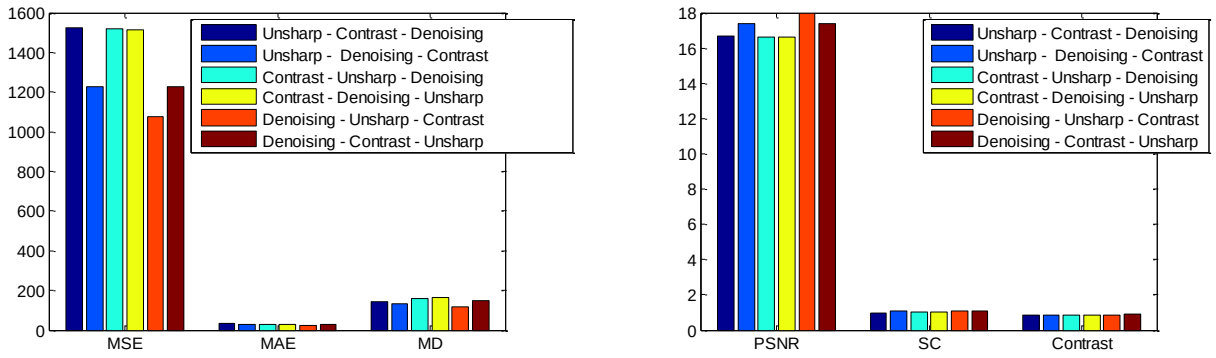

a) b)

Figure 11. Mean of image quality metrics for different combinations; a) MSE, MAE and MD; b) PSNR, SC and Contrast

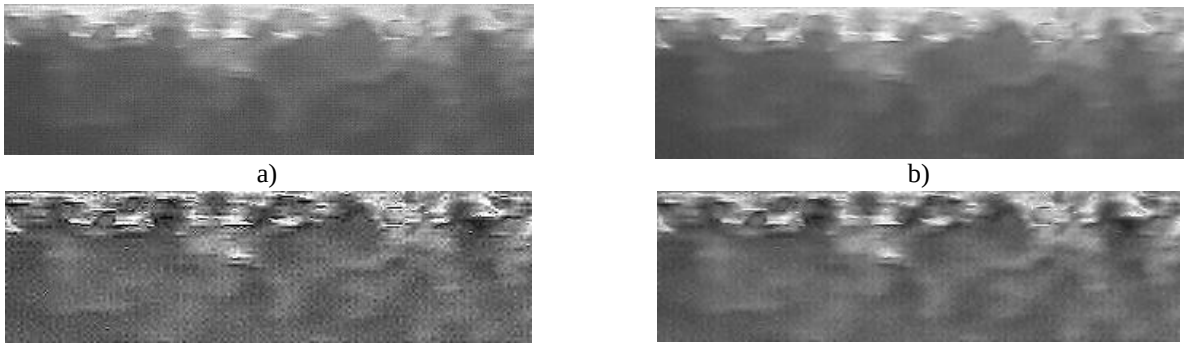

a) b)

c) d)

Figure 12. Visual enhancement results of different combinations for one image Uws=2.5 m/s, Uos=1.2 m/s; a) Original image; b) Original image after Wavelet denoising; c) Denoised image after unsharp filtering; d) Unsharped image after contrast improvement with CLAHE with Raylegh distribution

Figure 13. Flowchart of the proposed enhancement algorithm

4. CONCLUSIONS

Different methods for image enhancement have been reviewed, implemented and compared. Based on those methods a new methodology was proposed. Every method brings some benefit to the process, the Wavelet denoising reduces the noise preserving the edges, the unsharp filtering helps to emphasize texture and detail in the images and contrast enhancement improves the image contrast. The proposed method produces better results than the independent methods.

Different types of image quality metrics were implemented for getting the quality of each image; they presented good agreement with the visual result. A future work could compare the methods and the proposed method with some subjective metric.

5. ACKNOWLEDGEMENTS

The authors are grateful to CAPES (Coordenação de Aperfeiçoamento de Pessoal de Nível Superior) and PETROBRAS for the financial support.

6. REFERENCES

Angeli, P. and Hewitt, G.F. (1998), "Pressure gradient in horizontal liquid-liquid flows", *International Journal of Multiphase Flow*, Vol. 24 No. 7, pp. 1183–1203.

Arivazhagan, S., Deivalakshmi, S. and Kannan, K. (2007), "Performance Analysis of Image Denoising System for different levels of Wavelet decomposition", *International Journal of Imaging Science and Engineering*, Vol. 1 No. 3, pp. 104–107.

Bagade, S.S. and Shandilya, V. (2011), "Use of Histogram Equalization in Image Processing for Image Enhancement", *International Journal of Software Engineering Research & Practices*, Vol. 1 No. 2, pp. 6–10.

Boncelet, C. (2005), "Image Noise Models", *HANDBOOK OF IMAGE AND VIDEO PROCESSING*, Elsevier Inc., Second Edi., Vol. 2, pp. 397–409.

Donoho, D.L. and Johnstone, I.M. (1994), "Ideal Spatial Adaptation via Wavelet Shrinkage", *Biometrika*, Vol. 81, pp. 425–455.

Ergen, B. (2012), *Signal and Image Denoising Using Wavelet Transform*, (Baleanu, D.,Ed.)*Advances in Wavelet Theory and Their Applications in Engineering, Physics and Technology*, InTech, pp. 495–514.

Gonzales, R.C. and Woods, R.E. (2002), *Digital Image Processing*, Prentice Hall, Second edi.

Ioannou, K., Nydal, O.J. and Angeli, P. (2005), "Phase inversion in dispersed liquid–liquid flows", *Experimental Thermal and Fluid Science*, Vol. 29 No. 3, pp. 331–339.

Jin, F., Fieguth, P., Winger, L. and Jernigan, E. (2003), "Adaptive Wiener Filtering of Noisy Images and Image Sequences", *Image Processing, 2003. ICIP 2003. Proceedings. 2003 International Conference on*.

Juliastuti, E. and Epsilawati, L. (2012), "Image contrast enhancement for film-based dental panoramic radiography", *2012 International Conference on System Engineering and Technology (ICSET)*, Ieee, pp. 1–5.

Kaur, M., Kaur, J. and Kaur, J. (2011), "Survey of Contrast Enhancement Techniques based on Histogram Equalization", *International Journal of Advanced Computer Science and Applications*, Vol. 2 No. 7, pp. 137–141.

Lovick, J. and Angeli, P. (2004), "Experimental studies on the dual continuous flow pattern in oil–water flows", *International Journal of Multiphase Flow*, Vol. 30 No. 2, pp. 139–157.

Luisier, F., Blu, T. and Unser, M. (2007), "A new SURE approach to image denoising: interscale orthonormal wavelet thresholding.", *IEEE transactions on image processing : a publication of the IEEE Signal Processing Society*, Vol. 16 No. 3, pp. 593–606.

Omer, A. and Pal, R. (2010), "Pipeline Flow Behavior of Water-in-Oil Emulsions with and without a Polymeric Additive in the Aqueous Phase", *Chemical Engineering & Technology*, Vol. 33 No. 6, pp. 983–992.

Pal, R. (2007), "Mechanism of Turbulent Drag Reduction in Emulsions and Bubbly Suspensions", *Industrial & Engineering Chemistry Research*, Vol. 46, pp. 618–622.

Pavithra, P., Ramyashree, N. and Shruthi, T. V. (2010), "Image Enhancement by Histogram Specification Using Multiple Target Images", *Image (Rochester, N.Y.)*, Vol. 1 No. 2, pp. 3–5.

Rodriguez, I.H., Yamaguti, H.K.B., Castro, M.S. De and Silva, M.J. Da. (2011), "Drag Reduction Phenomenon in Viscous Oil-Water Dispersed Pipe Flow : Experimental Investigation and Phenomenological Modeling", *AIChE Journal*, Vol. 58 No. 9, pp. 2900–2910.

Singh, B., Mishra, R.S. and Gour, P. (2011), "Analysis of Contrast Enhancement Techniques For Underwater Image", *International Journal of Computer Technology and Electronics Engineering*, Vol. 1 No. 2.

Verma, R. and Ali, J. (2013), "A Comparative Study of Various Types of Image Noise and Efficient Noise Removal Techniques", *International Journal of Advance Research in Computer Science and Software Engineering*, Vol. 3 No. 10, pp. 617–622.

Yu, Y. and Acton, S.T. (2002), "Speckle Reducing Anisotropic Diffusion", *IEEE Transactions on Image Processing*, Vol. 11 No. 11, pp. 1260–1270.

7. RESPONSIBILITY NOTICE

The authors are the only responsible for the printed material included in this paper.